JKAU: Eng. Sci., **Vol 17** No. 2, pp: 19 - 40 (2006A.D. /1427 A.H.)

Fuzzy Algorithm for Supervisory Control of Self-Excited Induction Generator

Hussein F. Soliman, A. A. Attia*, S. M. Mokhymar, and M. A. L. Badr *****

*Currently Elect. &Computer Dept., Faculty of Eng., King Abdulaziz Univ., Jeddah, Saudi Arabia, and *National Research Institute of Astronomy and Geophysics & **Electricity & Energy Ministry New & Renewable Energy Authority, Wind Management*** & Elect. Power and Machine, Faculty of Engineering , Ain Shams Univ. Cairo, Egypt*

Abstract. This paper presents an application of Fuzzy Logic Controller (FLC) to regulate the reactive-power of the Self Excited Induction Generator (SEIG) driven by Wind Energy Conversion Schemes (WECS). The proposed FLC is used to tune the integral gain (K_I) of Proportional plus Integral (PI) controller. Two types of controls, for the generator and the wind turbine, using FLC algorithm have been introduced in this paper. The reactive-power control is performed to adapt the terminal voltage via self excitation. The active-power control is conducted to adjust the stator frequency through tuning the pitch angle of WECS blades. Both controllers utilize the Fuzzy technique to enhance the overall dynamic performance. The simulation result depicts a better dynamic response for the system under study during the starting period, and load variation. The percentage overshoot, rising time and oscillation are improved by the fuzzy controller compared to that with PI controller type.

1. Introduction

Many publications in the field of SEIG have been introduced to overcome different problems [e.g., enhancing the performance, loading, interfacing with the grid…etc]. Reference [1] discuses a method of control of 3 phase induction generator using the indirect field orientation control, while reference [2] introduces a FLC controller for wind energy utilization scheme. According to our survey there are no researches concentrating on a wind energy scheme system for supplying an isolated load. The primary advantages of SEIG are less maintenance cost, better transient performance, no need for dc power supply for field excitation, brushless construction (squirrel-cage rotor), etc. In addition, the induction generators have been widely employed to operate as wind-turbine generators and small hydroelectric generators of isolated power systems [3,4].

The connection of the induction generators to large power systems, to inject electric power, can be performed when the rotor speed of the induction generator is greater than the synchronous speed of the air-gap-revolving field. In this paper the dynamic performance is studied for SEIG driven by WECS to feed an isolated load. The d-q axes equivalent circuit model based on different reference frames extracted from fundamental machine theory can be employed to analyze machine transient's response in dynamic performance [3,4]. The reactive-power controller, for SEIG, is conducted to adapt the terminal voltage, via a semiconductor switching system. The semiconductor switch regulates the duty cycle which adjusts the value of capacitor bank connected to the SEIG [5, 6]. Also, the SEIG is equipped with an active-power controller to regulate the mechanical input power. In addition, the stator frequency is regulated. This is achieved by adjusting the pitch angle of wind turbine. In this paper the integral gain (K_i) of the PI controller is supervised using the FLC to enhance the overall dynamics response. The simulation results of the proposed technique are compared with the results obtained for the PI with fixed and variable K_i.

2. The System Under Study

Figure 1 shows the block diagram for the study system, which consists of SEIG driven by WECS connected to isolated load. Two control loops for terminal voltage and pitch angle using FLC to tune K_i of the PI controller are shown in the same figure. The mathematical model of SEIG driven by WECS is simulated using MATLAB / SIMULINK package to solve the differential mathematical equations. Meanwhile, two controllers have been developed for the system under study. The first one is the reactive-power controller to adjust the terminal voltage at the rated value. This is done by varying the switching capacitor bank, for changing the duty cycle, to adjust the self excitation. The second controller is the active-power controller to regulate the input power to the generator and thus maintain the stator frequency constant. This is achieved by changing the value of the pitch angle for the blade of the wind turbine. First, the system under study is tested when equipped with PI controller for both active and reactive-power controllers at different fixed values K_I. Then the technique is developed to drive the PI controller by a variable K_I to enhance the dynamic performance of the SEIG. The K_I is then tuned by using two different algorithms.

The simulation is carried out when the PI controller is driven by variable K_I using a linear function, with limitors, between K_I and voltage error for reactive control. Also, the simulation is include variable K_I based on the mechanical power error for active power controller. Meanwhile, the variable K_I has lower and upper limits. Then, the simulation is conducted when the PI controller is driven by a variable K_I through a FLC technique. The simulation results depict the variation of the different variables of the system under study, such as terminal voltage, load current, frequency, duty cycles of switching capacitor bank, variable K_I in reactive controller K_{IV} and variable K_I in active controller K_{IF}.

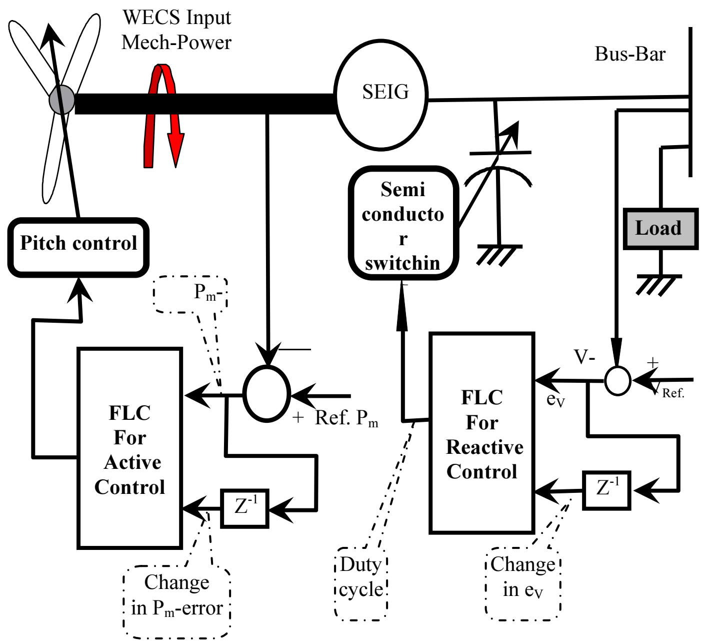

Fig. 1. System under study.

3. Mathematical Model of the SEIG Driven by WECS

3.1. Electrical Equation of the SEIG

The stator and rotor voltage equations, equation number (1) to (6) in Appendix-A, using Krause transformation [3,4], based on stationary reference frame. More details of the voltage equations are described in Ref. [7].

3.2. Mechanical Equations of the WECS

The mechanical equations relating the power coefficient of the wind turbine, tip speed ratio (μ) and pitch angle (β) are given in Ref. [7-9]. The analysis of an SEIG in this research is performed taking the following assumptions into account [3]:

- All parameters of the machine can be considered constant except X_m.
- Per-unit values of both stator and rotor leakage reactance are equal.
- Core loss in the excitation branch is neglected.
- Space and time harmonic effects are ignored.

3.3. Equivalent Circuit

The d and q axes equivalent-circuit models for the three-phase symmetrical induction generator are based on the equations given in Appendixes A and B. In addition, Appendixes C and D describe the other mathematical equations for the system under study. The equivalent-circuit parameters used in the simulation results refer to a 1.1 kW, 127/ 220 V (line voltage), 8.3/4.8 A (line current), 60 Hz, 2 poles, wound-rotor induction machine [4]. More details about the machine are descried in Ref. [7,8].

3.4. Reactive Power Control and Switching Capacitor Bank Technique

3.4.1. Switching

The switching of capacitors has been discarded in the past because of the practical difficulties involved [5,6], *i.e.*, the occurrence of voltage and current transients. It has been argued, and justly so, that current 'spikes' for example, would inevitably exceed the maximum current rating as well as the (di/dt) value of a particular semiconductor switch. The only way out of this dilemma would be to design the semiconductor switch to withstand the transient value at the switching instant.

The equivalent circuit in Fig. 2 is added to explain this situation of switching capacitor bank due to the duty cycle. The details of this circuit is given in Ref. [6]. For the circuit of Fig. 2, the switches are operated in anti-phase, *i.e.*, the switching function f_{s2} which controls switch S_2 is the inverse function of f_{s1} which controls switch S_1. In other words, switch S_2 is closed during the time when switch S_1 is open and vice versa. This mean that S_1 and S_2 of branch 1 and 2 are operated in such a manner that one switch is closed while the other is open.

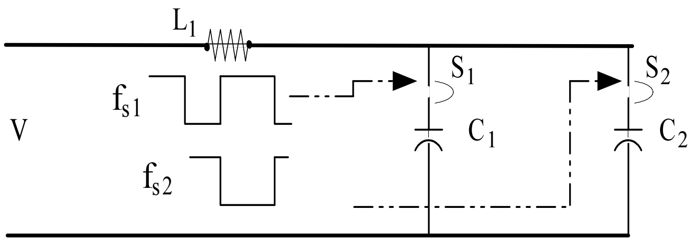

Fig. 2. Semi conductor switches (S_1,S_2) circuit for capacitor bank.

3.4.2. Reactive Power Control

As shown in Fig. 1, the input to the controllers is the voltage error while the output of the controllers is used to execute the duty cycle (λ). The value of calculated λ is used as an input to semiconductor switches to change the value of the capacitor bank according to the need for the effective value of the excitation. Accordingly, the terminal voltage is controlled by adjusting the self-excitation through automatic switching of the capacitor bank.

3.5. Active Power Control

Active power control is applied to the system under study by adjusting the pitch angle of the wind turbine blades. This is used to maintain the SEIG operating at a constant stator frequency and reject the effect of the speed disturbance. The pitch angle is a function of the power coefficient "C_p" of the wind turbine WECS. The value of C_p is calculated using the pitch angle value according to equations mentioned in Ref. [7-9]. Consequently, the best adjustment for the value of pitch angel leads to improve the mechanical power regulation, which, in turn, achieves a better adaptation for frequency of the overall system. Accordingly, the active power control regulates the mechanical power of the wind turbine.

4. Controllers

Two different types of controller strategies have been conducted. First, the application of the conventional PI controller with fixed and variable gains is carried out. Second, the application of FLC is used to adjust the value of K_I for both active and reactive controllers.

4.1. Conventional PI Controller

The simulation program is carried out for different values of K_I while the value of the proportional gain is kept constant as shown in Fig. 3. It is noticed from the simulation results that the value of percentage overshoot (P.O.S), rising time and settling time change as K_I is changed. Then the technique of having variable K_I depending on the voltage error, for reactive power control, is introduced to obtain the advantage of high and low value of the integral gain of voltage loop K_{IV}.

4.2. PI-Controller with Variable Gain

A program is developed to compute the value of the variable integral gain K_{IV} using the following rule based:

if ($e_V < e_{V\ min}$), $K_{IV} = K_{IV\ min}$;

elseif ($e_V > e_{V\ max}$), $K_{IV} = K_{IV\ max}$;

else ($e_{V\ min} < e_V < e_{V\ max}$),

$M = (K_{IV\ max} - K_{IV\ min}) / (e_{V\ max} - e_{V\ min})$; $C = K_{IV\ min} - M \times e_{V\ min}$;

$K_{IV} = M \times e_V + C$;

end

Where, e_V = the voltage error, $e_{V\ min}$= the minimum value of the voltage error, $e_{V\ max}$= the maximum value of the voltage error, $K_{IV\ min}$ is the minimum value of K_{IV}, $K_{IV\ max}$ is the maximum value of K_{IV}, C is a constant and M is the slop value. Figure 4 shows these rules based, to calculate the K_{IV} of the K_{IV} against the terminal voltage error e_V. The value of the $e_{V\ min}$ and $e_{V\ max}$ is obtained by trial and error to give the best dynamic performance.

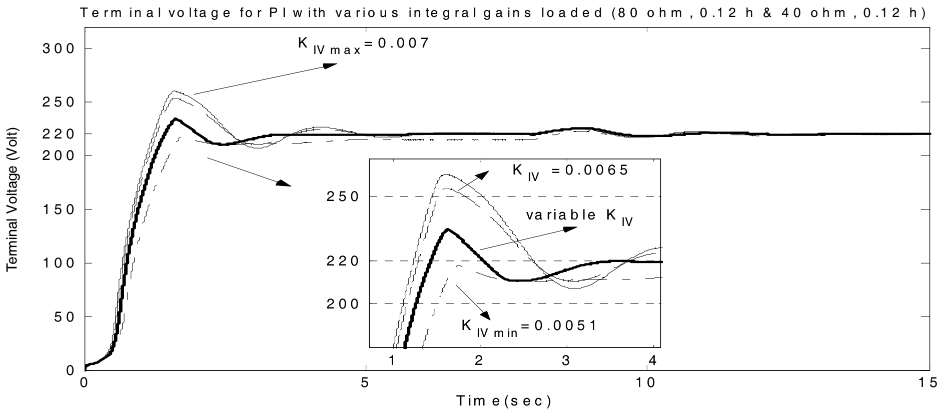

Fig. 3. Dynamic response of the terminal voltage with different values of integral gain for reactive controller.

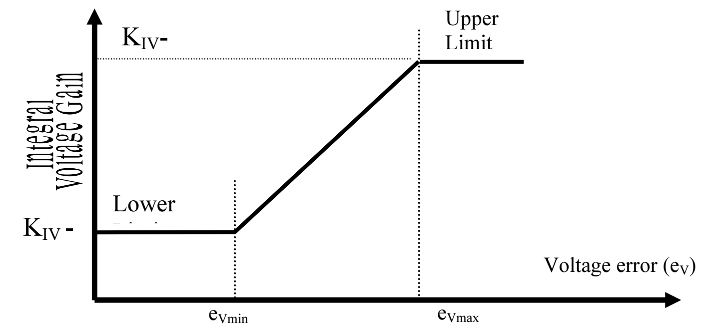

Fig. 4. Variable integral gain for pI controller.

Also, the proportional gains (K_{PV} and K_{PF}) are kept constant for the reactive and active controllers respectively. Various characteristics are tested to study the effect of changing the value of (K_{IV}) to update the reactive control. The simulation results cover the starting period and the period when the system is subjected to a sudden increase in the load, at instant 8 sec. Figure 3 shows the simulation results for the variable $K_{IV.}$ Figures 5&6 show the effect of variable reactive integral gain K_{IV} and active K_{IF} controllers versus time respectively.

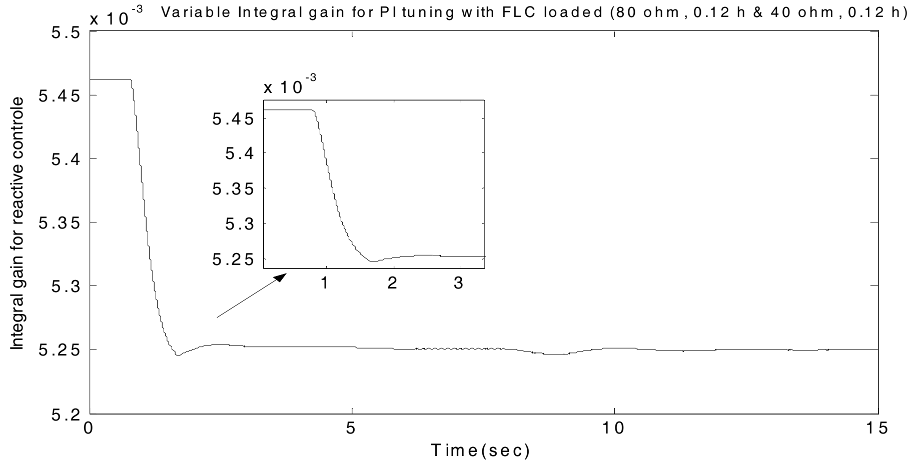

Fig. 5. Variable integral gain in PI-reactive controller with FLC.

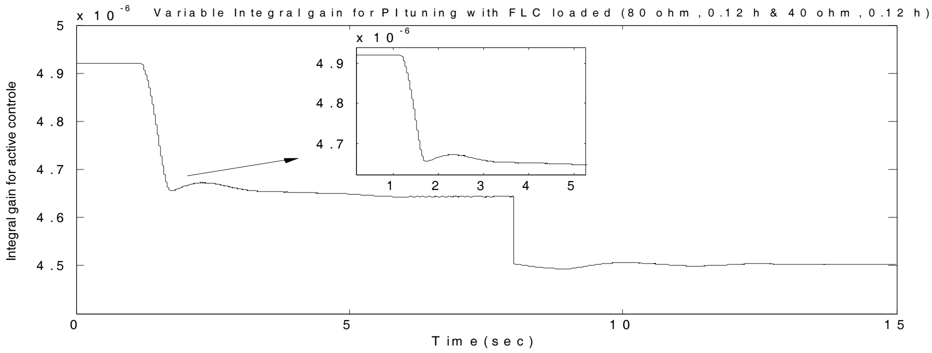

Fig. 6. Variable integral gain in PI-active controller with FLC.

5. A Fuzzy Logic Controller (FLC)

To design the fuzzy logic controller “FLC”, the control engineer must gather information on how the artificial decision maker should act in the closed-loop system, and this would be done from the knowledge base [10]. Fuzzy system is constructed from input fuzzy sets, fuzzy rules and output fuzzy sets, based on the prior knowledge base of the system. Figure 7 shows the basic construction of the FLC. There are rules to govern and execute the relations between inputs and outputs for the system. Every input and output parameter has a membership function which could be introduced between the limits of these parameters through a universe of discourse. The better adaptation of fuzzy set parameters the better tuning of the fuzzy output is conducted. The proposed FLC is used to compute and adapt the variable integral gain K_I of PI controller.

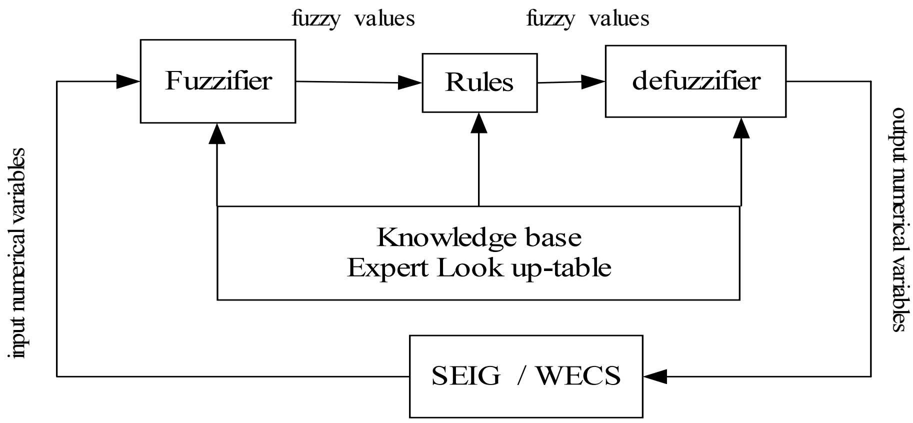

Fig. 7. The three stages of fuzzy logic controller .

5.1. Global Input and Output Variables

For reactive control the fuzzy input vector consists of two variable; first the terminal voltage deviation e_V and second is the change of the terminal voltage deviation Δe_V . Five linguistic variables are used for each of the input variables as shown in Fig. 8(a & b) respectively. While, the output variable fuzzy set is shown in Fig. 8(c & d) shows the fuzzy surface. Also, for active control the fuzzy input vector consists of two variable; first the mechanical power deviation e_F and second is the change of the mechanical power deviation Δe_F . Five linguistic variables are used for each of the input variables as shown in Fig. 9 (a) and Fig. 9 (b) respectively. While, the output variable fuzzy set is shown in Fig. 9 (c) and Fig. 9 (d) shows the fuzzy surface. In Fig. (8 & 9) a linguistic variables has been used, for input variables, P for Positive, N for Negative , AV for Average, B for Big and S for Small. For example PB is Positive Big and NS is Negative Small ….etc. After constructing the fuzzy sets for input and output variables it is required to develop the set of rules, so-called Look-up Table, which define the relation between the input variables, e_V, e_F, Δe_V and Δe_F and the output variable of the fuzzy logic controller. The output from fuzzy controller is the integral gain value of K_I used in the PI controller. The look-up Table is given in Table 1.

Table 1. Look up table.

Voltage Deviation (e_V)	Voltage Deviation Change (Δe_V)				
	NB	NS	AV	PS	PB
NB	NB	NB	NB	NS	AV
NS	NB	NB	NS	AV	PS
AV	NB	NS	AV	PS	PB
PS	NS	AV	PS	PB	PB
PB	AV	PS	PB	PB	PB

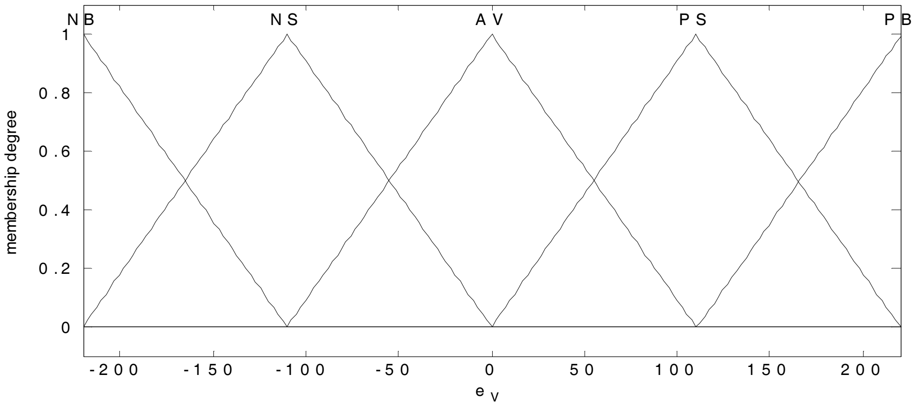

Fig. 8 (a). Membership function of voltage error.

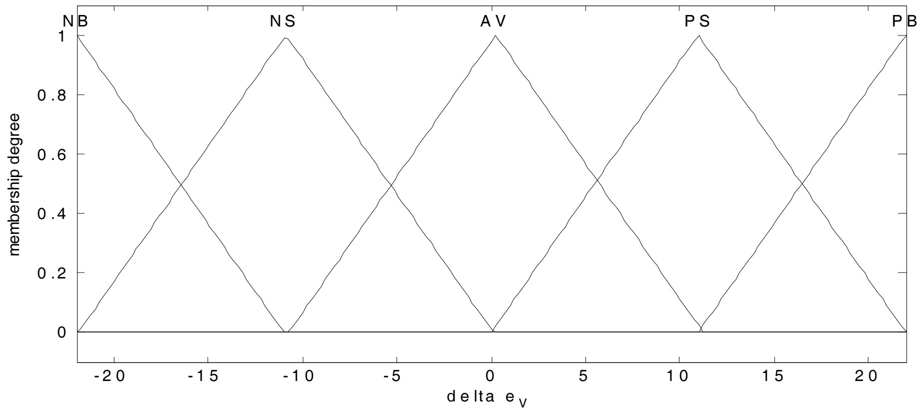

Fig. 8 (b). Membership function of change in voltage error.

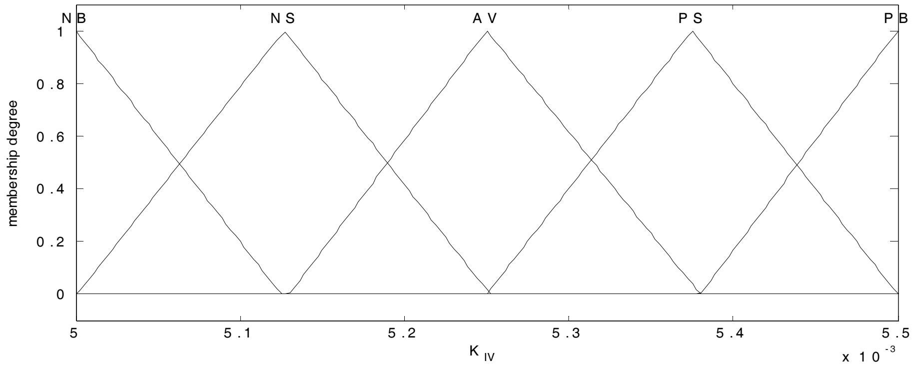

Fig. 8 (c). Membership function of variable K_{IV}.

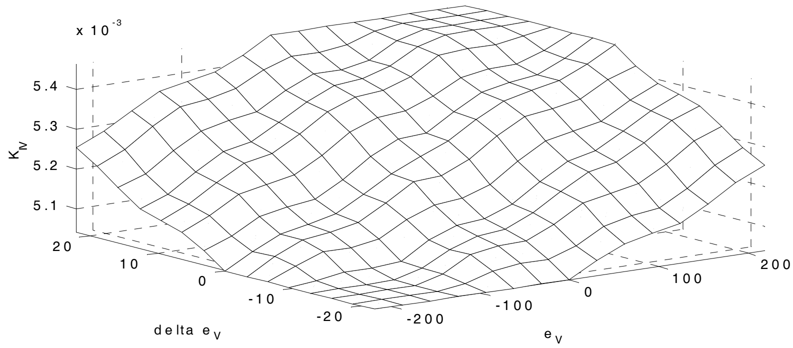

Fig. 8 (d) . Fuzzy surface.

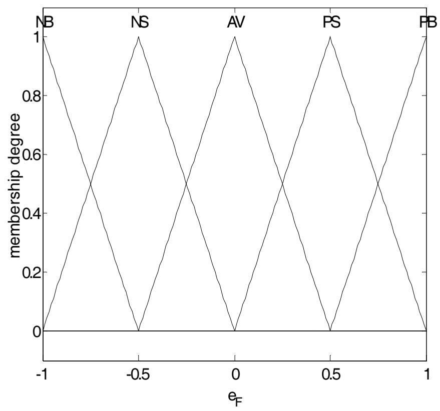

Fig. 9 (a). Membership function of mech. change power error.

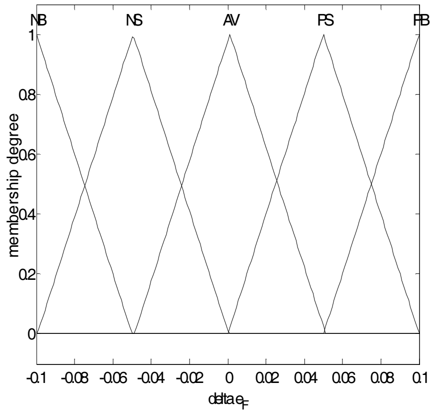

Fig. 9 (b). Membership function of on mech. power error.

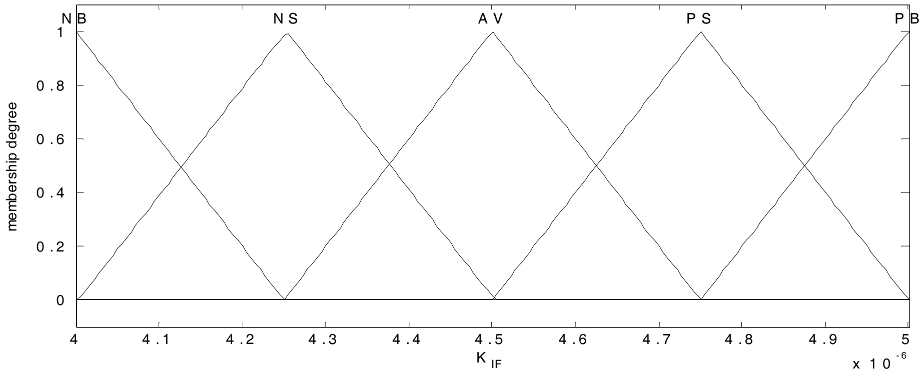

Fig. 9 (c). Membership function of variable K_{IF}.

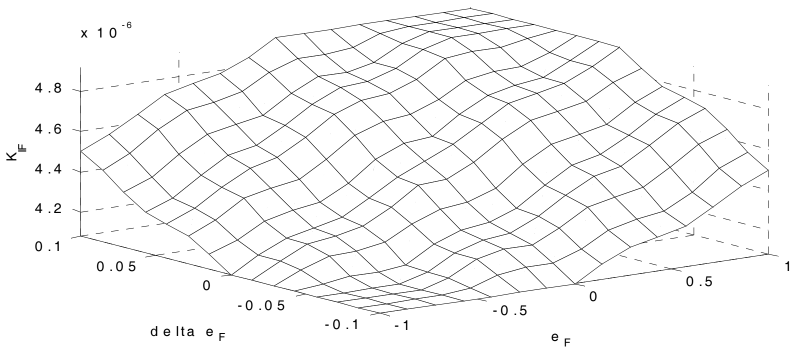

Fig. 9 (d). Fuzzy surface.

5.2. The Defuzzification Method

The Minimum of Maximum method has been used to find the output fuzzy rules representing a polyhedron map as shown in Fig. 10. First, the minimum membership grade, which is calculated from the min. value for the intersection of the two input variables (x_1 and x_2) with the related Fuzzy set in that rule. This min. membership grade is calculated to rescale the output rule, then the maximum is taken, as shown in Fig. 10. Finally, the centroid or center of area has been used to compute the fuzzy output, which represents defuzzification stage, as follows:

$$K_I = \frac{\int y \mu(y) dy}{\int \mu(y) dy}$$

More details about the variable of the above equation are given in Ref. [10].

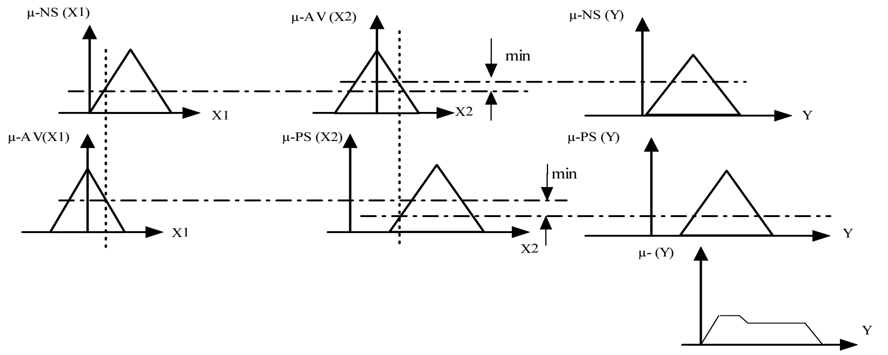

Rule1: if Verror (X1) is NS and Change in Verror (X2) is AV then output (integral gain (Y)) is NS
Rule2: if Verror (X1) is AV and Change in Verror (X2) is PS then output (integral gain (Y)) is PS

Fig. 10. Schematic diagram of the defuzzification method using the center of area.

6. Simulation Results

6.1. Dynamic Performance due to Suddenly Load Variation

The FLC utilizes the terminal voltage error (e_V) and its rate of change (Δe_V) as an input variables, to represent the reactive power control. The output of FLC is used to tune up the K_I of PI controller. Also, another FLC is used to regulate the mechanical power via the blade angle adaptation of the wind turbine. Figs. (8.a,b,c and d) depict the fuzzy sets of e_V, Δe_V , K_{IV} and fuzzy surface, respectively. The terminal voltage error (e_V) varies between (-220 and 220) and its change (Δe_V) varies between (- 22 and 22), and the output of the FLC is the K_{IV} which changes between (5e-003 and 5.5e-003). Table 1 shows the lookup table of fuzzy set rules for reactive control. The same technique is applied for active power controller where the two inputs for FLC are the mechanical power error (e_F) which varies between (-1 and 1) and its change (Δe_F)varies between (-0.1 and 0.1). The output of the FLC is the K_{IF} which changes between (4e-006 and 5e-006). The output of the PI-FLC in the active controller adapts the pitch angel value to enhance the stator frequency. Figure 9 (a,b, c & d) shows the fuzzy sets of e_F, Δe_F, the related output fuzzy set and fuzzy surface, respectively.

Based on the mathematical model of the system under study, equipped with two controllers (PI & FLC) for terminal voltage and blade angle, the simulation is carried out using the MATLAB- Simulink Package. Running for PI controller with various integral gain finding a relation between the voltage or frequency error and the value of this gains. Figures 11-13 show the simulation results for the terminal voltage for different loads, at time = 8 sec the system is subjected to sudden change in load. But Fig. 14 shows the stator frequency. The system is equipped with conventional controller having fixed and variable integral gain and FLC algorithm. The proposed FLC is used to adapt the K_I to give a better dynamic performance for the overall system, as shown in Fig. 11-13, regarding P.O.S and settling time compared with fixed PI and PI with variable K_I for different loads.

Also, Fig. 15 & 16 depict the simulation results for the load current and controller's duty cycle. The same conclusion is achieved as explained for Fig. 11.

6.2. Dynamic Performance due to Suddenly Wind Speed Variation

Another simulation result is conducted when the overall system is subjected to a sudden disturbance in the wind speed from 7 m/s to 15 m/s. in Fig. 17 & 18 show the simulation results of the wind speed variation and the stator frequency respectively. The simulation given in Fig. 18 shows the ability of the proposed controller to overcome the speed variation for variable and fixed integral gain.

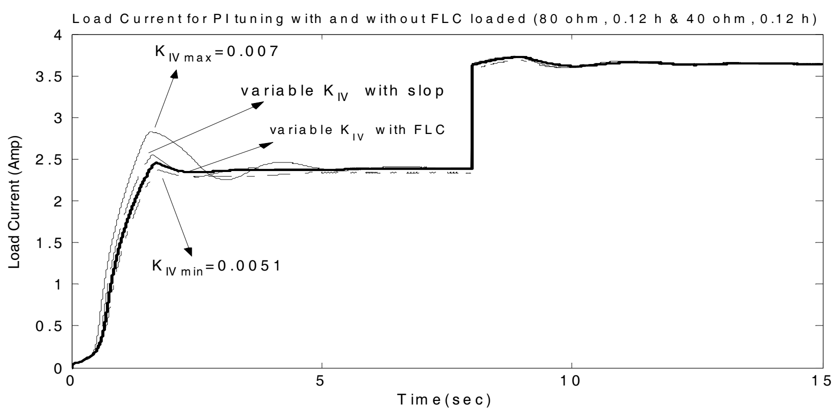

Fig. 11. Dynamic response of load current for PI with and without FLC.

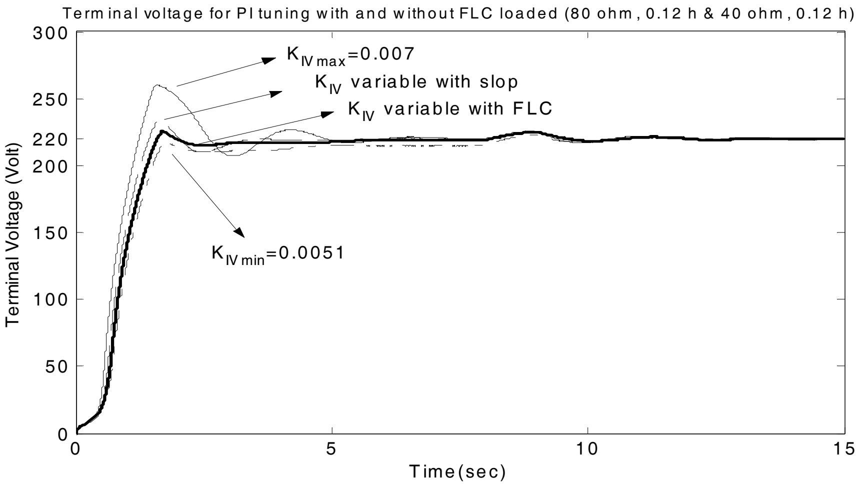

Fig. 11. Dynamic response of terminal voltage for PI with and without FLC.

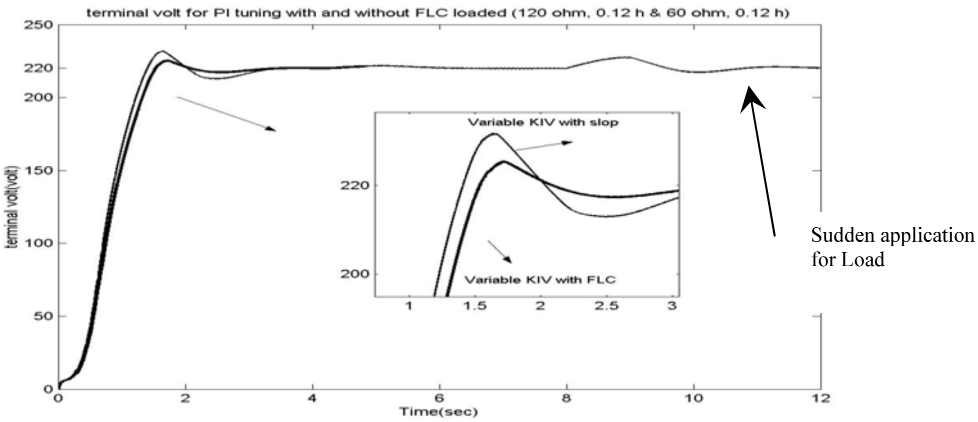

Fig. 12. Dynamic response of terminal voltage for PI with and without FLC.

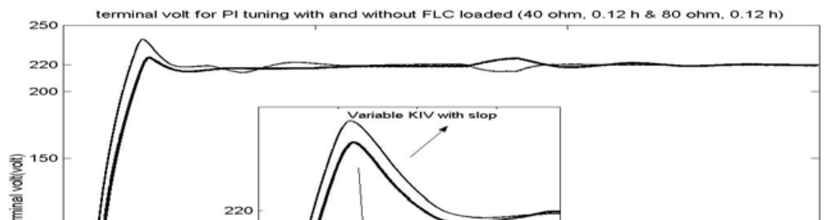

Fig. 13. Dynamic response of terminal voltage for PI with and without FLC.

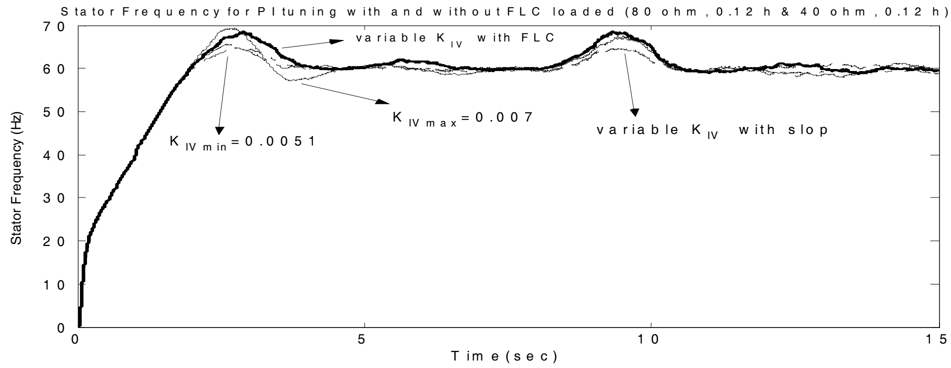

Fig. 14. Dynamic response of stator frequency for PI with and without FLC.

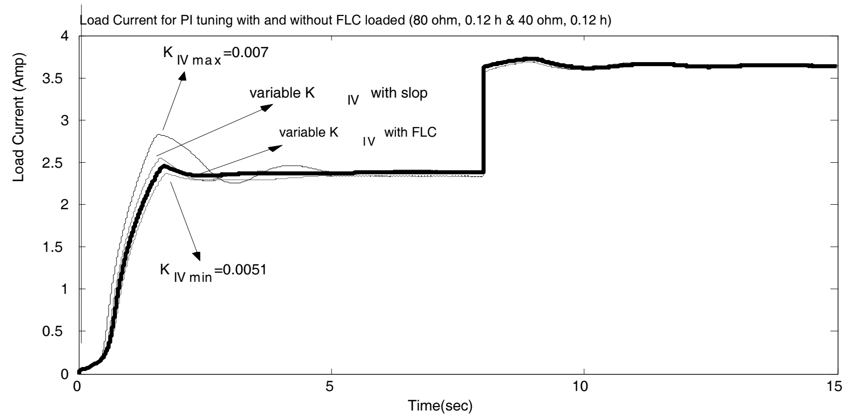

Fig. 15. Dynamic response of load current for PI with and without FLC.

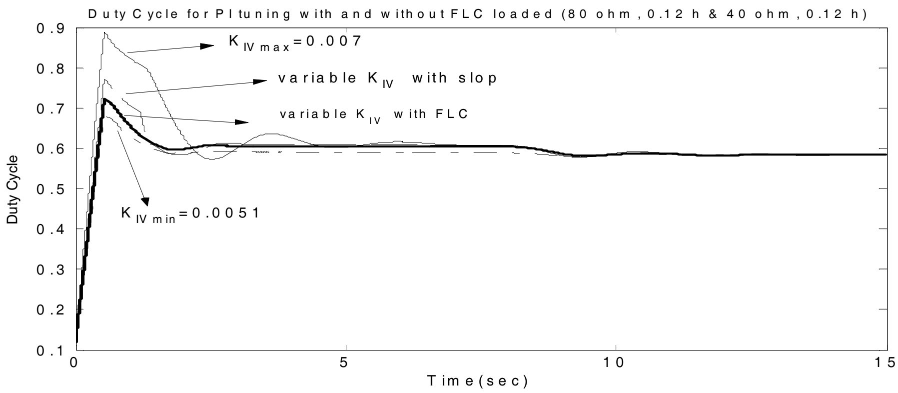

Fig. 16. Dynamic response of duty cycle for PI with and without FLC.

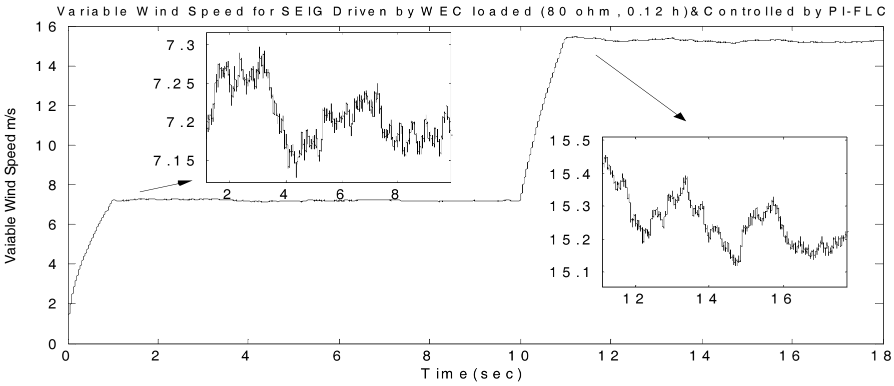

Fig. 17. Sudden variation for the wind speed versus time .

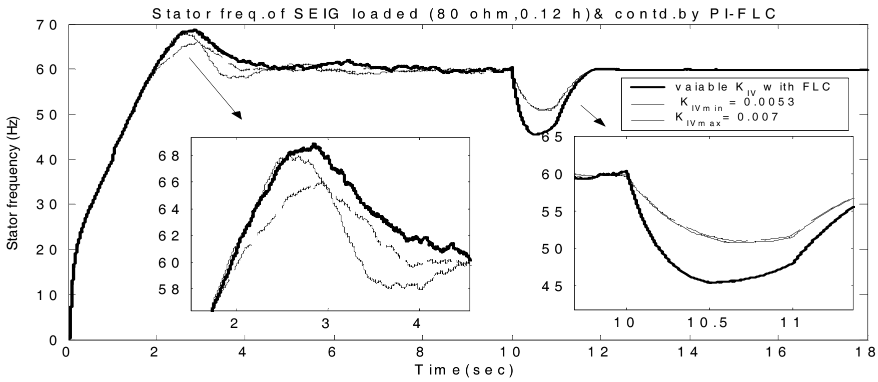

Fig. 18. Stator frequency according to the wind speed variation for SEIG controlled by FLC & PI.

7. Conclusion

This paper presents an application of FLC to self excited induction generator driven by wind energy. The proposed FLC is applied to active and reactive power controls of the system under study to enhance its dynamic performance. The FLC is used to regulate the duty cycle of the switched capacitor bank to adjust the terminal voltage of the induction generator. Another FLC is applied to regulate the blade angle of the wind energy turbine to control the stator frequency of the overall system. The simulation results show an enhancement of the dynamic performance of the overall system using the FLC controller compared with variable PI type. Another simulation is conducted to study the dynamic performance to this system with a suddenly disturbance for the wind speed variation. Where, a comparison is conducted for the stator frequency in the dynamic performance with variable and fixed K_I.

References

[1] **El_Sousy, F.,** **Orabi, M.** and **Godah, H.** "Indirect field orientation control of self-excited induction generator for wind energy conversion system" *ICIT*, **December** (2004).

[2] **Mashaly, A.M. S., Mansour, M.** and **Abd-Satar, A.A.**, " A fuzzy logic controller for wind energy utilization scheme", *Proceedings of the 3rd IEEE Conference of Control Application, Glasgow, Scotland, UK, August 24-26* (1994).

[3] **Li, Wang,** and **Jian-Yi-SU**, "Dynamic Performance of An Isolated Self Excited Induction Generator Under Various Loading Conditions", *IEEE Transactions on Energy Conversion*, **15** (1) March: 93-100 (1999).

[4] **Li, Wang** and **Lee, Ching- Huei,** "Long- Shunt and Short- Shunt Connections on Dynamic Performance of a SEIG Feeding an Induction Motor Load", *IEEE Transactions on Energy Conversion*, **14** (1): 1-7 (2000).

[5] **Atallah, A. M.** and **Ahmed, A.**,"Terminal Voltage Control of Slef Excited Induction Generators" *Sixth Middle-East Power Systems Conference (MEPCON'98), Mansoura, Egypt, Dec. 15-17*, pp: 110-118 (1998).

[6] **Marduchus, C.**, "Switched Capacitor Circuits for reactive power generation " , *Ph.D. Thesis*, Brunuel University (1983).

[7] **Hussein, F. S., Attia, A., Sabry, M., Badr M. M..A.L.** and **Ahmed, .A. E.M.S.**, "Dynamic Performance Enhancement of Self Excited Induction Generator Driven By Wind Energy Using ANN Controllers" *Sci. Bull. Fac. Eng. Ain Shams Univ*., ISSN 1110-1385, Part II, **39**(2) June 30: 631 -651 (2004).

[8] **Sabry, M.M.**, "Enhancement of The Performance of Wind Driven Induction Generators Using Artificial Intelligence Control", *Ph.D. Thesis*, Fac. Eng. Ain Shams Univ., March. 10, (2005).

[9] **Abdin, E. S.** and **Xu, Wilson**, "Control Design and Dynamic Performance Analysis of a Wind Turbine- Induction Generator Unit", *IEEE Transaction on Energy Conversion*, **15** (1) March: 91-96 (2000).

[10] **Passino, K.M.** and **Yurkovich, S.**, " *Fuzzy Control* ", Library of Congress Cataloging-in-Publication Data. Includes bibliographical references and index. ISBN 0-201-18074-X. Addison Wesley Longman, Inc. (1998).

Appendix (A)

SEIG differential equations at no load:

v_{ds} "Stator Voltage 's (volt) Differential Equation at Direct Axis"

$$V_{ds}=-R_s\cdot i_{ds}-\left(\frac{\omega}{\omega_b}\right)\left(-X_{ls}\cdot i_{qs}+x_m\left(i_{qr}-i_{qs}\right)\right)+p\left(\frac{\varphi_{ds}}{\omega_b}\right) \tag{A-1}$$

Where: i_{ds} is the stator current (amp) at direct axis, i_{qs} is the stator current at quadrant axis and i_{qr} : is the rotor current at quadrant axis.
X_l is the leakage reactance, s and r denoted for stator and rotor respectively. ω_b is the speed base. p is the differentiation parameter = d/dt.

v_{qs} "Stator Voltage 's Differential Equation at Quadrate Axis"

$$v_{qs}=-R_s\cdot i_{qs}+\left(\frac{\omega}{\omega_b}\right)\left(-X_{ls}\cdot i_{ds}+x_m\left(i_{dr}-i_{ds}\right)\right)+p\left(\frac{\varphi_{qs}}{\omega_b}\right) \tag{A-2}$$

Where: i_{dr} : is the rotor current (amp) at direct axis.

v_{dr} "Rotor Voltage 's Differential Equation at Direct Axis"

$$v_{dr}=R_r\cdot i_{dr}-\left(\frac{\left(\omega-\omega_r\right)}{\omega_b}\right)\left(X_{lr}\cdot i_{qr}+x_m\left(i_{qr}-i_{qs}\right)\right)+p\left(\frac{\varphi_{dr}}{\omega_b}\right) \tag{A-3}$$

Where: i_{qs} : is the stator current at quadrant axis.

v_{qr} "Rotor Voltage 's Differential Equation at Quadrate Axis"

$$v_{qr}=R_r\cdot i_{qr}+\left(\frac{\left(\omega-\omega_r\right)}{\omega_b}\right)\left(X_{lr}\cdot i_{dr}+x_m\left(i_{dr}-i_{ds}\right)\right)+p\left(\frac{\varphi_{qr}}{\omega_b}\right) \tag{A-4}$$

$$\frac{d\varphi_{qs}}{dt}=\omega_b\cdot\left(v_{qs}+R_s.i_{qs}-\varphi_{ds}\right) \tag{A-5}$$

Where: ω_b is the base speed.

$$\frac{d\varphi_{ds}}{dt}=\omega_b\cdot\left(v_{ds}+R_s.i_{ds}-\varphi_{qs}\right) \tag{A-6}$$

Appendix (B)

Magnetizing reactance & load case differential equations:

$$i_{ds}=\left(c\cdot\left(\frac{dv_{ds}}{dt}\right)\right)+\left[\left(v_{ds}-L_l\cdot\left(\frac{di_{Lds}}{dt}\right)\right)\Big/R_l\right] \tag{B-1}$$

$$i_{qs}=\left(c\cdot\left(\cdot\left(\frac{dV_{qs}}{dt}\right)\right)\right)+\left[\left(v_{qs}-L_l\cdot\left(\cdot\left(\frac{di_{Lqs}}{dt}\right)\right)\right)\Big/R_l\right] \tag{B-2}$$

$$i_m=\left(\left(i_{qr}-i_{qs}\right)^2+\left(i_{dr}-i_{ds}\right)^2\right)^{0.5} \tag{B-3}$$

$$T_e=\left[\varphi_{ds}\cdot\left(i_{qs}\right)-\varphi_{qs}\cdot\left(i_{ds}\right)\right] \tag{B-4}$$

$$x_m = [105.77] \ldots\ldots\ldots\ldots\ldots\ldots\ldots\ldots\ldots at\, 0.0 \le i_m < 0.864 \quad \text{(B-5)}$$

$$x_m = (340.2)/(i_m + 2.35) \ldots\ldots\ldots\ldots\ldots at\, 0.864 \le i_m < 1.051 \quad \text{(B-6)}$$

$$x_m = (227.4)/(i_m + 1.22) \ldots\ldots\ldots\ldots\ldots at\, 1.051 \le i_m < 1.476 \quad \text{(B-7)}$$

$$x_m = (202.3)/(i_m + 9.3) \ldots\ldots\ldots\ldots\ldots at\, 1.476 \le i_m < 1.717 \quad \text{(B-8)}$$

$$x_m = (179.8)/(i_m + 6.3) \ldots\ldots\ldots\ldots\ldots at\, 1.717 \le i_m \quad \text{(B-9)}$$

Appendix (C)

Excitation equations Differential equations:

$$i_{cd} = (c * p * \mathrm{v}_{cd} - \omega_s * C * \mathrm{v}_{cq}) \quad \text{(C-1)}$$

Where: ω_s is the synchronous speed (rad/sec) & i_{cd}: is the capacitor current in direct axis and i_{cq}: is the capacitor current in quadrant axis & C: is the value of the capacitor bank.

$$i_{cq} = (c * p * \mathrm{v}_{cq} + \omega_s * c * \mathrm{v}_{cd}) \quad \text{(C-2)}$$

$$\left(C * \frac{d\mathrm{v}_{ds}}{dt}\right) = (i_{ds} - i_{Lds}) \quad \text{(C-3)}$$

Where: I_{Lds} is the load current in direct axis and I_{Lqs}: is the load current in quadrant axis & R_L: is the load resistance (ohm) & L_L: is the load inductance (Henry).

$$\left(C * \frac{d\mathrm{v}_{qs}}{dt}\right) = (i_{qs} - i_{Lqs}) \quad \text{(C-4)}$$

$$(L_L * p i_{Lds}) = (\mathrm{v}_{ds} - R_L i_{Lds}) \quad \text{(C-5)}$$

$$(L_L * p i_{Lqs}) = (\mathrm{v}_{qs} - R_L i_{Lqs}) \quad \text{(C-6)}$$

$$\left(C * \frac{dV_{ds}}{dt}\right) = \left(i_{ds} - \left[V_{ds} - \left(L_L * \frac{di_{Lds}}{dt}\right) \Big/ R_L\right]\right) \quad \text{(C-7)}$$

$$\left(C * \frac{dV_{qs}}{dt}\right) = \left(i_{qs} + \left[V_{qs} - \left(L_L * \frac{di_{Lqs}}{dt}\right) \Big/ R_L\right]\right) \quad \text{(C-8)}$$

$$c_{eff} = \left[\frac{C_{\max}}{\left((1-\lambda)^2 + \sigma(\lambda)^2\right)}\right] \quad \text{(C-9)}$$

where C_{eff} : is the effective capacitor bank value (micro-farad), C_{max}: is the maximum capacitor value & C_{min}: is the minimum capacitor value & $\sigma = (C_{max} / C_{min})$ & λ: is the duty cycle value .

Appendix (D)

Mechanical Differential equations

$$\frac{d\omega_r}{dt} = (\omega_b/2H)(T_m - T_e - B.\omega_r) \tag{D-1}$$

where: ω_r is the rotor speed (rad/sec).

$$P_m = \left(\frac{1}{8}\right)\left(\pi\rho \;\; C_p D^2 V_w^3\right) \tag{D-2}$$

$$\omega_m = (2\ \pi n) / 60 \tag{D-3}$$

$$T_m = (P_m/\omega_m) \tag{D-4}$$

$$C_p = \left[\left(0.44 - 0.0167 \;\; \beta\right) \cdot Sin\left(\frac{\pi(\mu - 3)}{(15 - 0.3 * \beta)}\right) - 0.00184\ (\mu - 3)\beta\right] \tag{D-5}$$

$$\mu = \omega_m \left(\frac{R}{V_w}\right) = \left(\frac{D \;\; \pi \;\; n}{V_W \; 60}\right) \tag{D-6}$$

$$\frac{d\omega_r}{dt} = \left(\frac{\omega_b}{2H}\right)(T_m - T_e - B_a \cdot \omega_r) \tag{D-7}$$

Where: ω_m: is the mechanical speed (rad/sec)& P_m: is the mechanical power (KW) & T_m : is the mechanical torque (nm) & n : is the rotor revolution per minute (rpm) & C_p : is the power coefficient of the wind turbine & β : is the blade pitch angle (degree) & μ: is the tip speed ratio & V_w : is the wind speed (m/s) & R: is the of the rotor radius (m) of the wind turbine & D: is the of the rotor Diameter (m) of the wind turbine & B_a: is the friction factor & T_e: is the electrical torque (nm)& π = 3.14 & ρ = Air density (kg/m^3).

خوارزمية المنطق الغائم للتحكم الإشرافي في المولدات الحثية ذاتية الإثارة

حسين فريد السيد، وعبد الفتاح عطية*، و صبرى مخمير*، و محمد عبداللطيف بدر**

*قسم الهندسة الكهربائية والحاسب الآلي، كلية الهندسة، جامعة الملك عبد العزيز، جدة، المملكة العربية السعودية، * المعهد الوطني لبحوث الفلك والجيوفيزياء، حلوان، **وزارة الكهرباء والطاقة، هيئة الطاقة الجديدة والمتجددة، إدارة الرياح، *** قسم القوى الكهربائية والآلات، كلية الهندسة، جامعة عين شمس، القاهرة، مصر*

المستخلص. يتناول هذا البحث تحسين أداء المولد الحسي ذاتي الإثارة المدار بطاقة الرياح من خلال التحكم باستخدام نظام مهجن من النظام التكاملي التناسبي و نظام المنطق الغائم. وقد طُبقت تقنيتان للتحكم، التقنية الأولى تطبق من خلال الإثارة الذاتية لضبط جهد المولد عند قيمة ثابتة. والتقنية الثانية تتم من خلال التحكم في القدرة الميكانيكية الداخلة للمولد من توربينة الرياح وذلك بضبط سرعة الدوران باستخدام نظام الريش متغيرة الزاوية تحت سرعات رياح متغيرة، ومن ثم يتم ضبط تردد المولد عند قيمة ثابتة. وقد عنيت الدراسة بأداء المولد المعزول عن الشبكة عند حدوث تغير فجائي في الحمل المتصل به. حيث يتم ضبط قيمة المعامل التكاملي للنظام التكاملي التناسبي بواسطة طريقتين الأولى طريقة حسابية من خلال العلاقة الخطية بينه وبين قيمة الخطأ، والطريقة الأخرى تطبق نظام المنطق الغائم. كما تمت المقارنة بين منحنيات الأداء لكل من النظامين.